On Design Concept of Cellular Distributed MU-MIMO for Ultra-dense RAN

Fumiyuki Adachi†, Ryo Takahashi, Hidenori Matsuo
International Research Institute of Disaster Science, Tohoku University
468-1 Aoba, Aramaki, Aoba-ku, Sendai, Miyagi, 980-8572 Japan

Sijie Xia, Chang Ge, Qiang Chen
Department of Communications Engineering, Graduate school of Engineering, Tohoku University
6-6-05 Aoba, Aramaki, Aoba-ku, Sendai, Miyagi, 980-8579 Japan

† E-mail: fumiyuki.adachi.b4 @tohoku.ac.jp

2022 27th Asia Pacific Conference on Communications (APCC) | 978-1-6654-9927-9/22/$31.00 ©2022 IEEE | DOI: 10.1109/APCC55198.2022.9943686

***Abstract*—In 5G and beyond 5G systems, ultra-densification of radio access network (RAN) to improve the spectrum utilization efficiency is necessary due to continuously increasing mobile data traffic volume. Simple ultra-densification of RAN is not desirable since the problems of frequent handoff and severe interference will be caused. It is desirable to build the ultra-dense RAN based on the distributed multi-user multi-input multi-output (MU-MIMO) technology. In this paper, the design concept of cellular distributed MU-MIMO is presented to realize scalable ultra-dense RAN. In cellular distributed MU-MIMO, a wide communication service area is divided into a number of disjointed areas called cells using the distributed antenna location information and then, multiple user-centric small cells called user-clusters are formed in each cell using the user location information. To effectively mitigate intra- and inter-cell interferences caused by RAN ultra-densification, fully and semi-decentralized interference coordination (IC) schemes are presented.**

Keywords—RAN, cellular system, distributed MIMO, 5G-advanced, beyond 5G

I. Introduction

The 5th generation (5G) mobile communication systems [1],[2] have been put into service operation worldwide in around 2020. Since then, the research and development efforts have been intensified to realize 5G-advanced systems [3] and beyond 5G systems [4]. Mobile data traffic is increasing at a compound annual growth rate (CAGR) of approximately 46% [5]. It is necessary to further improve the spectrum utilization efficiency as well as utilize the mmWave band, where wider frequency bandwidths remain unused.

One of the important features of cellular systems is to deploy a number of base stations (BSs) over a wide communication service area and to reuse the same frequency at different BSs in order to reduce the transmit power of user terminals and to efficiently utilize the limited available frequency bandwidth [6]. The spectrum utilization efficiency can be improved by dense deployment of BSs. This is called the densification of the radio access network (RAN). However, such a simple RAN densification is not desirable since frequent handoff (switching BS to continue the communication) is caused. Furthermore, severe interference is caused, thereby limiting the improvement in the spectrum utilization efficiency.

In 5G, mmWave band e.g. 28GHz, where wider bandwidth is available than below 6GHz bands, is used. However, mmWave signals have a strong rectilinear propagation property and thus, the signal propagation paths are frequently blocked by obstacles e.g. buildings between the transmitter and receiver. This blockage problem of mmWave signals must be considered when addressing the RAN densification.

In this paper, we present the design concept of cellular distributed MU-MIMO based on the distributed multi-user multi-input multi-output (MU-MIMO) technology [7]. In cellular distributed MU-MIMO, a wide communication service area is divided into a number of geographically disjointed areas called cells using the distributed antenna location information and then, multiple user-centric small cells called user-clusters are formed in each cell using the user location information. The user-clustering is introduced to improve the spectrum utilization efficiency by MU-MIMO technology and dense frequency reuse, while the cellular structuring is introduced to ensure the RAN scalability by restricting the radio signal processing of each BS to users in its cell area. In cellular distributed MU-MIMO systems, severe intra- and inter-cell interferences are caused, thereby limiting the improvement of spectrum utilization efficiency. In this paper, fully decentralized and semi-decentralized interference coordination (IC) schemes that can effectively mitigate these interferences are presented.

This paper is organized as follows. In Chapter II, two possible approaches toward RAN ultra-densification are presented. Chapter III presents the design concept of cellular distributed MU-MIMO. In Chapter IV, our recent work on IC schemes in cellular distributed MU-MIMO systems is introduced.

II. Approaches Toward RAN Ultra-densification

For convenience, we refer to the coverage area of BS in 4G systems as the macro cell. An effective approach to improve the spectrum utilization efficiency is to deploy a massive number of small cell BSs (i.e., to realize a small cell network) in the macro cell area. However, such a simple RAN ultra-densification results in frequent handoff to continue the communication while users are moving. Therefore, the control signaling traffic will increase, thereby reducing the system capacity to provide data services. In order to effectively improve the spectrum utilization efficiency while alleviating frequent handoff problem, there will be two possible approaches based on MU-MIMO technology.

A. RAN densification based on MU-MIMO technology

Two possible approaches based on MU-MIMO technology are shown in Fig. 1. One is co-located MU-MIMO approach, in which an array antenna consisting of a massive number of antenna elements is placed at a BS site to form narrow beams toward users located in the macro cell area. The other is distributed MU-MIMO approach, which distributes a massive number of antennas each with the radio part (frequency conversion, radio signal power amplifier, etc.) over the macro cell area.

In both MU-MIMO approaches, the radio signal processing, communication data processing, and radio control and management functions remain at the BS site. Distributed antennas are connected to the BS via optical mobile fronthaul. RAN using distributed MU-MIMO is similar to a centralized

RAN (C-RAN) [8] and a cell-free massive MIMO [9] deployed in a macro cell area.

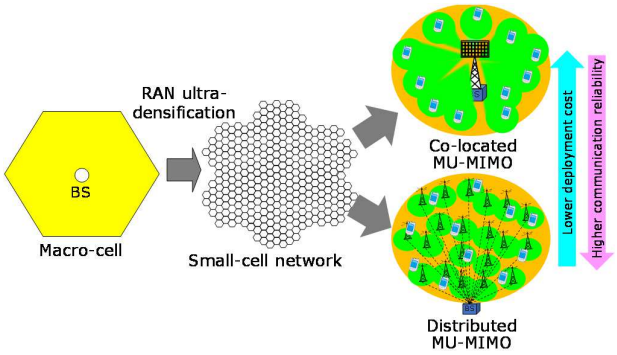

Fig.1 Approaches toward RAN ultra-densification.

B. Cluster-wise distributed MU-MIMO

Regardless of whether it is co-located or distributed, a large-scale MU-MIMO requires radio signal processing of a prohibitively high computational complexity. To remedy this problem, we form user-clusters by grouping together neighborhood users that cause strong interference to each other and then, select a relatively small number of antennas (or beams) for each user-cluster. By doing so, a computationally demanding large-scale MU-MIMO can be replaced with reduced-computational complexity small-scale cluster-wise MU-MIMO. However, there still remains a problem. In 5G, the mmWave band is adopted. The mmWave signals have a rectilinear propagation property and frequent blockage will happen due to obstacles e.g. buildings located between transmitter and receiver. This frequent blockage can be alleviated by distributing antennas over the area. As a consequence, cluster-wise distributed MU-MIMO can be the best approach for the ultra-densification of RAN.

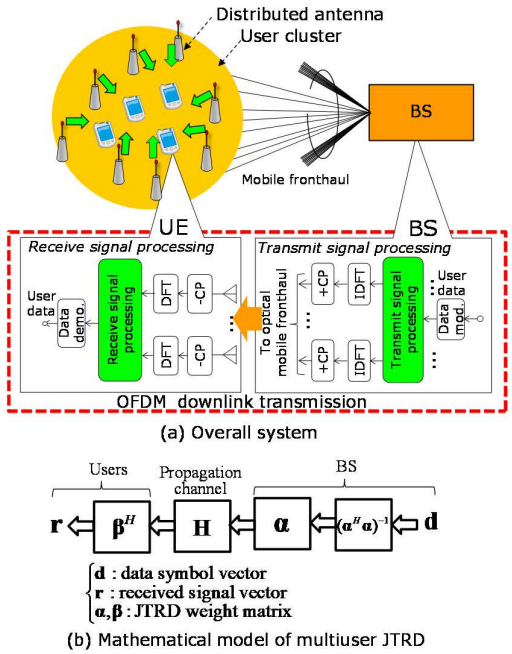

Fig. 2 Downlink transmission system model of cluster-wise distributed MU-MIMO.

The downlink transmission system model of cluster-wise distributed MU-MIMO employing multi-user joint transmit-receive diversity (JTRD) scheme [10], [11] is illustrated in Fig. 2. Fig. 2(a) is an overall system model assuming OFDM and Fig. 2(b) is a mathematical model (represented in the matrix form) of zero-forcing (ZF) based multi-user JTRD. Distributed antennas can be either a single antenna or an array antenna. In Fig. 2(b), $\mathbf{H}$ represents the multi-user MIMO channel matrix between distributed antennas and users in a user-cluster of interest, $\boldsymbol{\alpha}$ and $\boldsymbol{\beta}$ respectively represent JTRD weight matrices at BS andtotality of users, and a concatenation of $\boldsymbol{\alpha}$ and $\left(\boldsymbol{\alpha}^H\boldsymbol{\alpha}\right)^{-1}$ constitutes the ZF precoder which removes the multi-user interference in a user-cluster of interest. $\boldsymbol{\alpha}$ and $\boldsymbol{\beta}$ can be obtained by either singular-value decomposition (SVD) of the channel associated with each user or solving eigen-equation composed of the channel correlation matrix associated with each user.

III. Design Concept

A. Conceptual architecture

The conceptual architecture of cellular distributed MU-MIMO is illustrated in Fig. 3. Instead of directly configuring user-cluster structure over the entire wide communication service area, the service area is firstly divided into a number of geographically disjointed areas called cells. Then, under the condition of configured cellular structure, user-cluster structure is configured in each cell. The RAN controller is responsible for determining the number of cells in the service area and for configuring the cellular structure using the location information of distributed antennas, while each BS is responsible for configuring the user-cluster structure using the location information of users in its cell and for performing cluster-wise distributed MU-MIMO (see Sect. II).

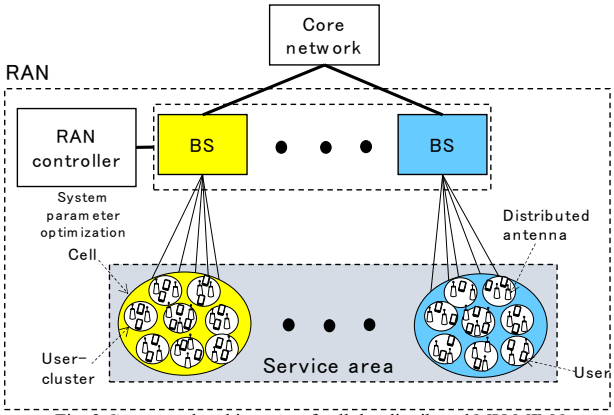

Fig. 3 Conceptual architecture of cellular distributed MU-MIMO.

The above procedure to configure the user-centric small cell structure over the service area is introduced to realize a scalable and flexible ultra-dense RAN by keeping the radio signal processing power required for each BS within a feasible value while keeping it uniform among different BSs. As the signal processing power of BS improves, the number of cells can be reduced, bringing the system closer to a cell-free system.

B. Cellular structuring and user-cluster forming

MU-MIMO signal transmission requires antennas equal to or greater than the number of users to be spatially multiplexed (assuming one stream transmission per user). A constrained K-means algorithm [12] is used to configure the cellular structure and to form user-clusters, respectively. The constraints used for configuring the cellular structure are the

number of cells and the maximum allowable number of distributed antennas in each cell, while the constraints for configuring the user-cluster structure are the number of user-clusters in each cell and the maximum number of users in each user-cluster [13]. A larger number of distributed antennas must be deployed in urban areas than in suburban areas. The cell size becomes smaller in an urban area than in a suburban area. Even in an urban area, distributed antennas must be more densely deployed in shopping and business areas and accordingly, cell size becomes much smaller.

Fig. 4 shows an example of configured cell/user-cluster structure for the cases of uniform distribution and non-uniform distribution of antennas/users [13]. A total of 3,200 single-antenna users are distributed over the area with a higher density in the central region. A total of 3,200 antennas are distributed over the area according to the user density. It is assumed that BS has the radio signal processing power to perform cluster-wise distributed MU-MIMO of spatially multiplexing up to 8 users each for 16 user-clusters. Therefore, the number of distributed antennas required is set to 128. Accordingly, the maximum number of users in each cell becomes 128 (=16×8). Cells are formed by the constrained K-means algorithm with a constraint of 128 antennas, resulting in 25 (=3200/128) cells in the service area. The average number of users per cell becomes 128 (=3,200/25) and approximately 16 (=128/8) user-clusters are formed in each cell.

Since user locations will change due to user mobility, it is necessary to update user-clusters periodically. In the case of a small cell network (as shown in Fig. 1), handoff process is initiated not to discontinue the communication when a user moves into a new small cell area. However, in the case of distributed/co-located MU-MIMO, since the radio signal processing is carried out at each BS, the communication can be continued without the need of handoff as far as a user stays in the same BS cell area. Handoff occurs only when a user moves across the BS cell boundary.

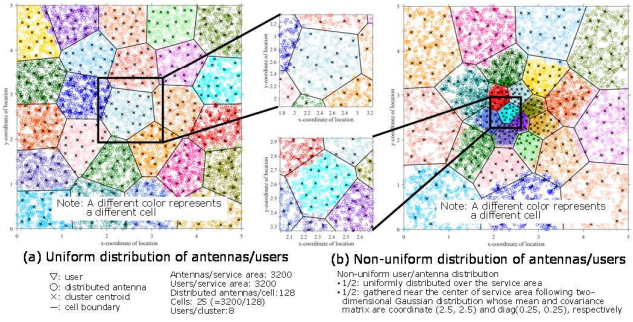

Fig. 4 An example of cell/cluster structure.

It should be noted that if the BS signal processing power is sufficiently high, a single BS can cover a wide communication service area, thus enabling a cell-free communication system. Furthermore, by virtualizing a large number of BSs as a cloud RAN using cloud computing, the cellular structure can be flexibly reconfigured according to changes in the status of deployed distributed antennas.

IV. IC FOR CELLULAR DISTRIBUTED MU-MIMO

A. Intra- and inter-cell interferences

In a cellular distributed MU-MIMO communication system, when cluster-wise distributed MU-MIMO is performed using the same frequency at all BSs, intra-cell interference and inter-cell interference occur (Fig. 5). This limits the improvement in spectrum utilization efficiency that can be achieved by RAN densification. In order to deal with the interference problem, some effective intra-cell and inter-cell IC schemes are required.

The well-known inter-cell IC scheme is fractional frequency reuse (FFR) [14]. In FFR, a different fractional bandwidth is allocated to users in the cell-edge region of a different neighborhood cell, as shown in Fig. 6. The other bandwidth is allocated to the inner-cell region. This is an example of frequency-domain scheduling (see the above figure in Fig. 6(b)), in which communication opportunities are allocated to users in the inner-cell and cell-edge regions simultaneously. Time-domain scheduling is also possible (see the bottom figure in Fig. 6(b)). Both scheduling schemes are equivalent in terms of spectrum utilization efficiency, but frequency-domain scheduling is considered more suitable for low latency communications.

Intra-cell IC is performed in a decentralized manner by each BS. On the other hand, inter-cell IC is performed either in a decentralized manner by each BS or in a centralized manner by the RAN controller. This paper describes inter- and intra-cell IC schemes.

The interference comes from other user-clusters of own cell and surrounding cells. Lowering the transmit power in distributed MU-MIMO can reduce interference. Therefore, transmit power control is also an important issue in IC. We have been studying the optimal transmit power allocation for distributed MU-MIMO [15].

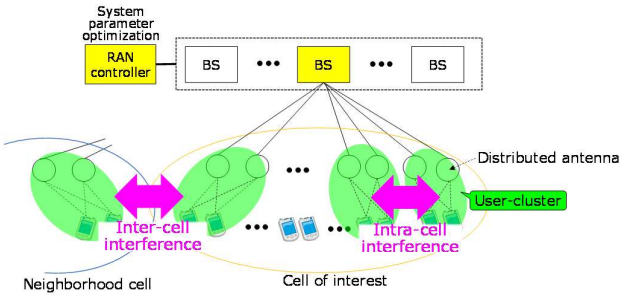

Fig. 5 Intra-cell interference and inter-cell interference.

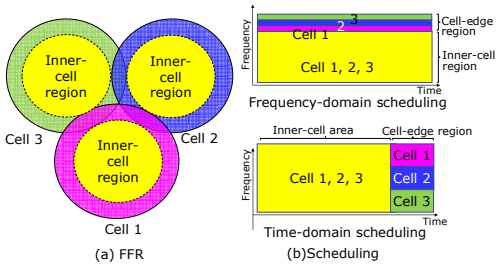

Fig. 6 FFR-based inter-cell IC and scheduling.

B. Fully decentralized IC scheme

Intra-cell and inter-cell IC schemes are based on cluster multilayering, the basic idea of which is schematically shown in Fig. 7.

The control parameter for intra-cell IC is the interference offset distance (IOD). First, user-clusters are formed based on the predetermined number of users per user-cluster and the user location information. Then, in order to reduce the intra-cell interference, user-clusters are divided into several layers

so that user-clusters in the same layer can be separated from each other by a distance greater than or equal to IOD [16], [17].

1) Cluster multilayering

Simple cluster multilayering reduces the number of clusters placed in the lower layers. Accordingly, the lower the layer, the greater than IOD the distance between user-clusters becomes, thereby limiting the spectrum utilization efficiency improvement. Therefore, to remedy this problem, some of user-clusters are placed in different layers multiple times as far as the IOD requirement is satisfied.

Even when the IOD requirement is satisfied, users may still experience strong intra-cell interference from neighborhood user-clusters in the same layer. Those users are called cluster-edge users. Also users close to cell boundaries (called cell-edge users) are subject to strong inter-cell interference from the neighborhood cells. Such cluster-edge and cell-edge users are treated as low quality users and are placed also in the bottom layer called low-quality layer while being kept in their original user-clusters [18].

Fig. 7 shows an example of the above-mentioned multi-layered clustering. The simulation setting is the same as in Sect. III B. Three layers are constructed. The bottom layer is the low-quality layer, in which cell-edge and cluster-edge users are placed together. ▽ and ○ in Fig. 7 represent distributed antennas and users, respectively. 16 user-clusters are formed in a cell. For the sake of clarity, a circle with a radius R, which is half the average distance between neighborhood clusters is drawn in the figure. The IOD is set to $2R$. As can be seen from the placement of user-clusters in each layer, the inter-cluster distance is larger than $2R$, thereby reducing intra-cell interference. Cell-edge users and cluster-edge users placed in the bottom layer, i.e., low-quality layer, are indicated by pink and green colors, respectively. Note that they also remain in their original user-clusters placed in the 1st and 2nd layers.

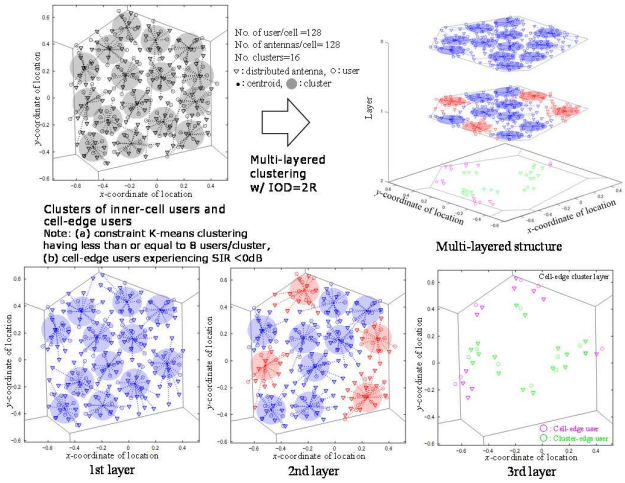

Fig. 7 Example of cluster multilayering.

In the low-quality layer, FFR-based inter-cell IC is applied to the cell-edge users and the remaining bandwidth is allocated to the cluster-edge users. It should be noted that a group of cell-edge users and that of cluster-edge users are spatially multiplexed respectively by cluster-wise distributed MU-MIMO. Also noted is that the communication opportunity is given to each layer in turn by round-robin time-domain scheduling and that the cell-edge and cluster-edge users are also given the communication opportunity when layers above the low-quality layer in which they are placed are given the communication opportunity.

2) FFR with best 2 sub-bands segregation algorithm

The inter-cell IC is applied to the cell-edge users placed in the low-quality layer (the bottom layer in Fig. 7). We applied the channel segregation (CS) algorithm [19] to realize adaptive FFR which can adapt to the propagation environment. The CS-FFR is designed to allocate the best sub-band to cell-edge users of each cell. Recently, we have extended the CS-FFR so as to allocate the best 2 sub-bands to cell-edge users of each cell [18].

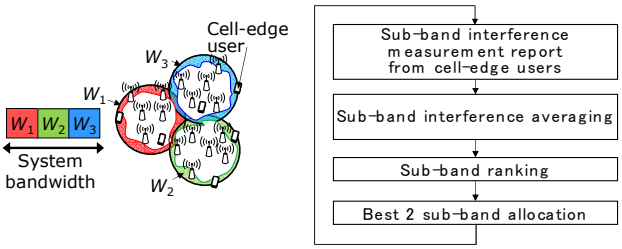

(a) FFR with 3 sub-bands (b) CS-FFR procedure at each BS

Fig. 8 CS-FFR with the best 2 sub-bands allocation.

Fig. 8 shows the procedure of a CS-FFR with the best 2 sub-bands allocation. Each BS can allocate the best 2 sub-bands to its cell-edge users in a decentralized manner, thus realizing a highly adaptive and scalable RAN. In CS-FFR with the best 2 sub-bands allocation, the cell-edge users measure their received inter-cell interference levels and report them to their BS, and then, BS determines the best 2 sub-bands with the lowest average inter-cell interference levels and allocates them to its cell-edge users. This process is iterated. According to our simulation [18], the CS-FFR with the best 2 sub-bands allocation converges after around 100 iterations.

3) User capacity evaluation

The downlink user capacity is evaluated by computer simulation to confirm the effectiveness of the fully decentralized IC scheme. Here, as a preliminary evaluation, instead of using multi-user JTRD described in Sect. II for cluster-wise distributed MU-MIMO, we consider the minimum mean square error filtering combined with singular value decomposition (MMSE-SVD) [20] assuming single-antenna users. Uniformly distributed antennas and users are considered. Simulation setting for other parameters is the same as in Sect. III. The propagation channel is modelled as distance-dependent pathloss with pathloss exponent of 3.5, log-normally distributed shadowing loss with standard deviation of 7dB, and Rayleigh fading. Shadowing loss and fading for all propagation channels between users and distributed antennas are assumed to be independent, respectively. Assuming a service area of the normalized size of 5×5 (see Fig. 4), the transmit power for each user is set so that the received signal-to-noise ratio (SNR) becomes 0 dB at a receiver location whose distance is $1/\sqrt{2}$ from the transmitter. Thus, the considered cellular distributed MU-MIMO system is interference-limited. Up to 8 users having the received signal-to-interference ratio (SIR) below 0 dB are classified as the cell-edge users and the cluster-edge users, respectively, depending on the cause of interference. Then, 2 distributed antennas are selected for each user for performing cluster-wise distributed MU-MIMO in the low-quality layer.

The cumulative distribution function (CDF) of the downlink user capacity with fully decentralized IC scheme for users in the central cell is plotted in Fig. 9. For comparison, the user link capacities achievable without IC and with single-antenna transmission/reception (user-wise SISO) are also plotted. It can be seen from Fig. 9 that the cellular distributed MIMO with cluster-wise distributed MU-MIMO significantly improves the link capacity compared to the user-wise SISO case (no MU-MIMO) even when IC is not utilized and further improves the link capacity by using fully decentralized IC, in particular, for the low capacity region.

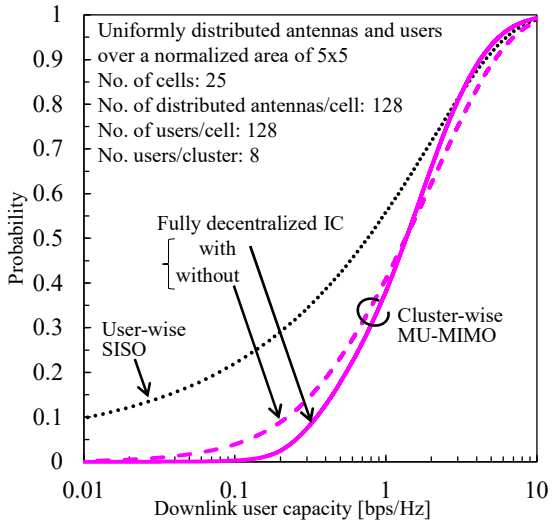

Fig. 9 Downlink capacity.

C. Semi-decentralized IC scheme

In semi-decentralized IC, the RAN controller carries out the FFR-based inter-cell IC in a centralized manner, while each BS performs intra-cell IC in a decentralized manner. The inter-cell IC is carried out first, followed by the intra-cell IC. Recently, we proposed such a semi-decentralized IC scheme using the graph coloring algorithm (GCA) [21].

The system bandwidth is divided into several subbands having equal bandwidth. Here, each subband is represented by a different color. The whole set of colors (i.e., system bandwidth) is then divided into several color sub-sets. RAN controller allocates one of sub-sets to each BS so that each BS can color its cell-edge clusters by itself. Note that, different from a fully decentralized IC scheme, user-clusters in each cell are classified into two types of the cluster: inner-cell cluster and cell-edge cluster. The minimum number of colors in each sub-set is 2. An example of a whole set and sub-sets of colors when a total number of colors is 8 is shown in Fig. 10.

Figure 11 schematically depicts the flow of a semi-decentralized IC scheme, which consists of two steps, i.e., GCA-FFR-based inter-cell IC and GCA-based intra-cell IC under the condition of the inter-cell IC result.

Step 1 (GCA-FFR) is carried out by the RAN controller. After the cell structure is configured by constrained K-means algorithm using the location information of distributed antennas as presented in Sect. III B, Delaunay triangulation [22] is done using the location information of the cell-centroids to create a graph. Then, one of the color sub-sets (4 sub-sets in Figs. 10 and 11) is allocated to each cell using the largest degree order-based GCA (LDO-GCA) [23]. Note that responsible for coloring the cell-edge clusters using colors in the sub-set allocated by the RAN controller is each BS in Step 2.

In Step 2, each BS colors the cell-edge clusters as follows. Each BS creates a graph by carrying out Delaunay triangulation using the location information of the cluster-centroids in its own cell. Then, BS finds a convex hull and colors the corresponding clusters as cell-edge clusters by using colors in the color sub-set which has been already allocated by the RAN controller in Step 1. Since the cell-edge clusters are in a row along the cell edge, a simple round-robin coloring can be used, in which BS picks up one color from the color sub-set in turn. However, note that, when the number of cell-edge clusters is odd, the colors of the first and last user-clusters collide since they are neighbors. Avoiding such a color collision is our future study. Next, under the condition that the cell-edge clusters corresponding to the convex hull have already been colored, each BS colors its inner-cell clusters using LDO-GCA.

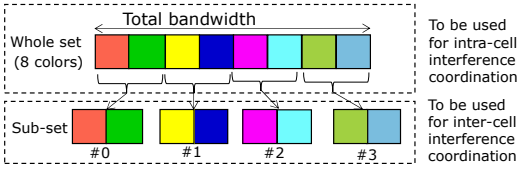

Fig. 10 Whole set and sub-sets of colors.

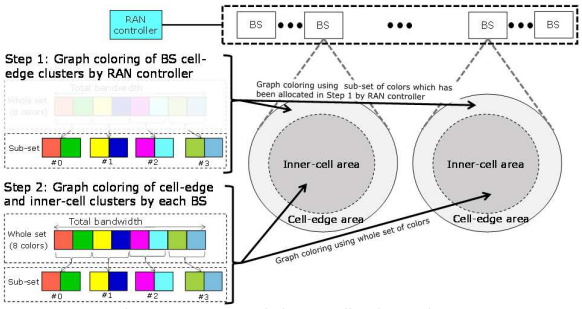

Fig. 11 2-step semi-decentralized IC scheme.

1) Coloring of cell-edge clusters by LDO-GCA

Fig. 12 shows an example of the coloring result of cell-edge clusters after Step 1 (LDO-GCA using 4 sub-sets of 2 colors each) and Step 2 (round robin coloring), assuming a uniform distribution of 3,200 users and 3,200 distributed antennas over the area. Cell structure is configured as shown in Sect. III B. Assuming 128 users in each cell, 16 user-clusters are formed in each cell by a constrained K-means algorithm. It can be seen from Fig. 12 that the cell-edge clusters facing each other at the cell boundary are colored differently from each other and therefore, the strong inter-cell interference can be mitigated.

2) Coloring of inner-cell clusters by DSATUR-GCA

Fig. 13 shows an example of the coloring result of inner-cell clusters for the cell indicated by the black circle in Fig. 12. LDO-GCA with the whole set of 8 colors is used. For comparison, we also show a coloring result of inner-cell clusters using the degree of saturation (DSATUR)-GCA [24]. Note that LDO-GCA has an advantage of lower computational complexity than DSATUR-GCA.

Reinforcement learning coloring algorithm (RLCA) [25] can be used to directly color clusters in a cell. Since RLCA

does not require a graph, it is more adaptable to various propagation environments than LDO-GCA. However, it is computationally expensive, so reducing its computational complexity is an issue for the future.

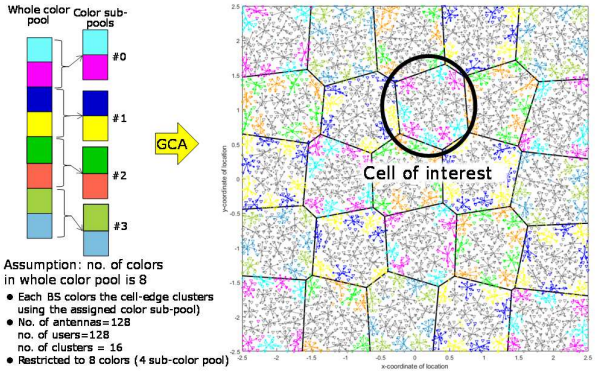

Fig.12 An example of cell-edge clusters coloring result.

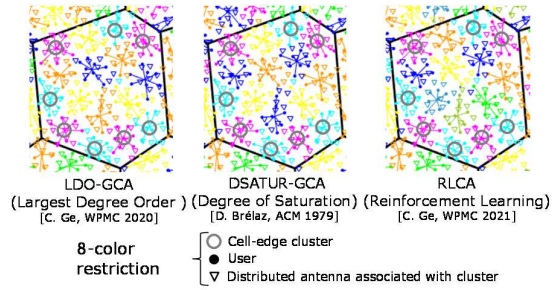

Fig. 13 An example of inner-cell clusters coloring result.

V. Conclusions

This paper presented the design concept of a cellular distributed MU-MIMO which can improve the spectrum utilization efficiency while mitigating effectively the severe interference caused by RAN densification. The cellular distributed MU-MIMO is designed to reconfigure cellular/user-cluster structure according to changes in the communication environment due to user mobility and addition/deletion (or on/off) of some of the distributed antennas. The reconfigurability of the cell/user-cluster structure enables scalable and flexible ultra-dense RAN.

A detailed evaluation of the cell/user-cluster reconfigurability and the interference mitigation effect of fully/semi-decentralized IC schemes is left for our future study. In this paper, we assumed that the perfect information of antenna locations and that of user locations are available at the RAN controller and at each BS, respectively. However, obtaining the user location information is hard, in particular, in the case of indoor areas. How to form user-clusters in such a situation is left as an important issue. Finally, it should be pointed out that a reconfigurable cellular distributed MU-MIMO cannot be realized without the reconfigurability in optical mobile fronthaul. Further advancement of optical mobile fronthaul is highly expected.

Acknowledgment

A part of this work was conducted under "R&D for further advancement of the 5th generation mobile communication system" (JPJ000254) commissioned by the Ministry of Internal Affairs and Communications in Japan.

References

[1] P. Marsch, et al, "5G Radio Access Network Architecture: Design Guidelines and Key Considerations," IEEE Com. Mag., Vol.54, Issue 11, Nov. 2016.
[2] A. Benjebbour, K. Kitao, Y. Kishiyama, and C. Na, "3GPP Defined 5G Requirements and Evaluation Conditions," NTT DOCOMO Tech. J., Vol. 19, No. 3, pp. 13-23, Jan. 2018.
[3] T. Murakami, et al, "Research Project to Realize Various High-reliability Communications in Advanced 5G Network," Proc. IEEE WCNC 2020, Seoul, Korea, 25-28 May 2020.
[4] G. Gui, M. Liu, F. Tang, N. Kato, and F. Adachi, "6G: Opening New Horizons for Integration of Comfort, Security, and Intelligence," IEEE Wireless Com., Vol. 27, Issue 5, pp. 126-132, Oct. 2020.
[5] Cisco Visual Networking Index: Global Mobile Data Traffic Forecast Update, 2017–2022.
[6] W.C. Jakes, *Microwave Mobile Communications*, IEEE Press, 1993.
[7] L. Sanguinetti and H. V. Poor, "Fundamentals of Multi-user MIMO Communications," Chap.6 in V. Tarokh, Ed., *New directions in wireless communications research*, Springer, Aug. 2009.
[8] 3GPP TS 36.300, "Evolved Universal Terrestrial Radio Access (E-UTRA) and Evolved Universal Terrestrial Radio Access Network (E-UTRAN), Overall description," Ver. 12.10, Jan 2017.
[9] H. I. Obakhena, A. L. Imoize1, F. I. Anyasi and K. V. N. Kavitha, "Application of Cell-free Massive MIMO in 5G and Beyond 5G Wireless Networks: A Survey," J. Eng. Appl. Sci., Vol. 68, No. 13, Oct. 2021.
[10] F. Adachi and R. Takahashi, "User-wise Joint Transmit-receive Diversity for Multi-user MIMO," Proc. ICETC 2020, 2-4 Dec. 2020.
[11] F. Adachi and R. Takahashi, "On Understanding of Massive MIMO Beam-forming From Multi-user Joint Transmit-receive Diversity Principle," IEEE VTC2021-Spring, Helsinki, Finland, 25-28 April 2021.
[12] P. Bradley, K. Bennett and A. Demiriz, "Constrained K-Means Clustering", Microsoft Research Technical Report, May. 2000.
[13] S. Xia, C. Ge, Q. Chen, and F. Adachi, "Cellular Structuring and Clustering for Distributed Antenna Systems," Proc. WPMC 2021, Okayama, Japan, 14-16 Dec. 2021.
[14] M. Qian, et al., "Adaptive Soft Frequency Reuse Scheme for Wireless Cellular Networks," IEEE Trans. VT, Vol.64, Issue 1, pp.118-131, Jan. 2015.
[15] S. Xia, C. Ge, Q. Chen, and F. Adachi, "Optimal Power Allocation for Cluster-wise Distributed MU-MIMO System," Proc. IEEE VTC2021-Fall, 27-30 Sept. 2021.
[16] F. Adachi, R. Takahashi, and H. Matsuo, "Enhanced Interference Coordination and Radio Resource Management for 5G Advanced Ultra-dense RAN," Proc. IEEE VTC2020-Spring, 25-28 May 2020.
[17] R. Takahashi and F. Adachi, "Performance of Enhanced Interference Coordination Using Multi-layered Clustering for 5G Advanced Ultra-dense RAN," Proc. IEEE VTC2021-Spring, Helsinki, Finland, 25-28 April 2021.
[18] R. Takahashi, H. Matsuo, and F. Adachi, "Scalable and Reconfigurable Distributed MU-MIMO System," Proc. IEEE VTC2022-Spring, Workshop W13: TPoC6G 2022, Helsinki, Finland, 19 June, 2022.
[19] K. Temma, F. Adachi, L. Shan, Y. Owada, K. Hattori, and K. Hamaguchi, "Convergence Analysis of Interference-aware Channel Segregation," IEICE ComEX, Vol.6, No.7, 460-466, July 2017.
[20] Y. Seki and F. Adachi, "Improving link capacity by multi-user MMSE-SVD with ICI information in a distributed MIMO cellular network," IEICE Communications Express, Vol. 7, Issue 9, pp. 316-321, Sept. 2018.
[21] C. Ge, S. Xia, Q. Chen, and F. Adachi, "2-Step Graph Coloring Algorithm for Cluster-wise Distributed MU-MIMO in Ultra-dense RAN," Proc. WPMC 2020, 19-26 Oct. 2020.
[22] J. Keil and C. Gutwin, "Classes of Graphs Which Approximate the Complete Euclidean Graph," Discrete and Computational Geometry, Vol. 7, No. 1, pp. 13–28, 1992.
[23] C. Ge, S. Xia, Q. Chen, and F. Adachi, "Graph Coloring-based Interference Coordination for Ultra-dense Cellular Network with Distributed MU-MIMO," Proc. IEEE VTC2021-Fall, 27-30 Sept. 2021.
[24] D. Brélaz, "New Methods to Color the Vertices of a Graph," Communications of the ACM, Vol.22, Issue 4, pp. 251-256, Apr. 1979.
[25] C. Ge, S. Xia, Q. Chen, and F. Adachi, "Reinforcement Learning-based Interference Coordination for Distributed MU-MIMO," Proc. WPMC 2021, Okayama, Japan, 14-16 Dec. 2021.